NIH Public Access
Author Manuscript
Biochimie. Author manuscript; available in PMC 2014 May 01.

Published in final edited form as:
Biochimie. 2013 May ; 95(5): 1023–1032. doi:10.1016/j.biochi.2013.02.003.

The C-terminal domain of CblD interacts with CblC and influences intracellular cobalamin partitioning☆

Carmen Gherasim[a,1], **Luciana Hannibal**[b,1], **Deepa Rajagopalan**[a], **Donald W. Jacobsen**[b,c,d,**], and **Ruma Banerjee**[a,*]

[a]Department of Biological Chemistry, University of Michigan Medical Center, Ann Arbor, MI 48109-0600, USA

[b]Department of Cellular and Molecular Medicine, Lerner Research Institute, Cleveland Clinic, Cleveland, OH 44195, USA

[c]School of Biomedical Sciences, Kent State University, Kent, OH 44242, USA

[d]Department of Molecular Medicine, Cleveland Clinic Lerner College of Medicine, Case Western Reserve University, Cleveland, OH 44106, USA

Abstract

Mutations in cobalamin or B_{12} trafficking genes needed for cofactor assimilation and targeting lead to inborn errors of cobalamin metabolism. The gene corresponding to one of these loci, *cbl*D, affects both the mitochondrial and cytoplasmic pathways for B_{12} processing. We have demonstrated that fibroblast cell lines from patients with mutations in CblD, can dealkylate exogenously supplied methylcobalamin (MeCbl), an activity catalyzed by the CblC protein, but show imbalanced intracellular partitioning of the cofactor into the MeCbl and 5′-deoxyadenosylcobalamin (AdoCbl) pools. These results confirm that CblD functions downstream of CblC in the cofactor assimilation pathway and that it plays an important role in controlling the traffic of the cofactor between the competing cytoplasmic and mitochondrial routes for MeCbl and AdoCbl synthesis, respectively. In this study, we report the interaction of CblC with four CblD protein variants with variable N-terminal start sites. We demonstrate that a complex between CblC and CblD can be isolated particularly under conditions that permit dealkylation of alkylcobalamin by CblC or in the presence of the corresponding dealkylated and oxidized product, hydroxocobalamin (HOCbl). A weak CblC·CblD complex is also seen in the presence of cyanocobalamin. Formation of the CblC·CblD complex is observed with all four CblD variants tested suggesting that the N-terminal 115 residues missing in the shortest variant are not essential for this interaction. Furthermore, limited proteolysis of the CblD variants indicates the presence of a stable C-terminal domain spanning residues ~116–296. Our results are consistent with an adapter function for CblD, which in complex with CblC·HOCbl, or possibly the less oxidized CblC·cob(II)alamin, partitions the cofactor between AdoCbl and MeCbl assimilation pathways.

☆This work was supported by grants from the National Institutes of Health (DK45776 to RB and HL71907 to DWJ) REFER MS Set As per style.

© 2013 Published by Elsevier Masson SAS.

*Corresponding author. University of Michigan, Biological Chemistry, 1150 W. Medical Center Dr., Ann Arbor, MI 48109-5606, USA. Tel.: +1 734 615 5238, rbanerje@umich.edu (R. Banerjee). **Corresponding author. Department of Cellular and Molecular Medicine, NC-10, Lerner Research Institute, Cleveland Clinic, 9500 Euclid Ave. Cleveland, OH 44195, USA. Tel.: +1 216 444 8340. jacobsd@ccf.org (D.W. Jacobsen).
[1]Equal contributors

NIH-PA Author Manuscript
NIH-PA Author Manuscript
NIH-PA Author Manuscript

NIH-PA Author Manuscript

NIH-PA Author Manuscript

NIH-PA Author Manuscript

Keywords

Cobalamin; Traffic; Homocystinuria; B_{12}

Although only two human enzymes use cobalamin (or derivatives of B_{12}) as a cofactor, its intracellular handlers are many [1,2]. Clinical genetics studies have led to the recognition of at least seven loci (*cbl*A–F and *cblJ*) that support B_{12} functions in addition to the two encoding the B_{12}-dependent enzymes, methionine synthase (*cbl*G) and methylmalonyl-CoA mutase (*mut*) [3-5]. With the recent identification of all seven genes encoding proteins dedicated to intracellular B_{12} assimilation and trafficking [6-13], elucidation of their biochemical functions has just begun, providing early insights into a complex intracellular pathway for B_{12} processing. Given the relative rarity of the B_{12} cofactor (30–700 nM in human tissues [14]) and its reactivity in all three biologically relevant cobalt oxidation states, we have proposed that navigation of cobalamin from its point of exit from the lysosome to its destinations in the cytoplasm (methionine synthase) and mitochondrion (methylmalonyl-CoA mutase) respectively, relies on protein escorts [1,2]. B_{12} trafficking can be classified into (i) the early or common pathway, (ii) the methylcobalamin (MeCbl) branch and (iii) the 5′-deoxyadenosylcobalamin (AdoCbl) branch (Fig. 1). Functions in the early pathway are shared for assimilation of MeCbl and AdoCbl needed by methionine synthase and methylmalonyl-CoA mutase, respectively and include the *cbl*F, *cblJ*, *cbl*C and *cbl*D loci. Defects in these loci typically lead to combined methylmalonic aciduria and homocystinuria, as expected for impaired activity of both B_{12} enzymes. Defects in the MeCbl branch (*cbl*G and *cbl*E) lead to isolated homocystinuria whereas mutations in the AdoCbl branch (*cbl*A, *cbl*B and *mut*) lead to isolated methylmalonic aciduria. The exception to this tidy classification is the *cbl*D locus, which shows complexity, in that depending on the location of the pathogenic mutation, patients exhibit either combined or isolated methylmalonic aciduria and homocystinuria [15]. The CblD protein is predicted to have an eleven-residue mitochondrial leader sequence at the N-terminus [9,16]. Mutation analyses reveal that defects at the N- and C-termini of the encoded CblD[2] protein are associated with methylmalonic aciduria and homocystinuria respectively, suggesting that either different isoforms or distinct protein domains support the MeCbl versus the AdoCbl branches of the pathway [9,16]. Initiation codons at positions 1, 62 and 116 in good Kozak contexts are located on the mRNA encoding CblD, supporting the possibility that internal initiation sites can be used to produce CblD variants [16]. However, western blot analysis reveals the presence of only full-length CblD protein in wild-type human fibroblasts [16]. In contrast, the shorter variants corresponding to initiation at the 62 and 116 start sites were seen in fibroblasts from a patient with homozygous nonsense mutation that results in termination of CblD at Ser20. Hence, internal initiation at Met62 and Met116 is likely to be important in a subset of *cbl*D patients with mutations that result in premature termination of the protein impacting AdoCbl synthesis but allowing MeCbl synthesis [16].

CblD belongs to an uncharacterized protein family with limited sequence similarity to the ATPase component of a putative ABC transporter [9]. However, CblD is missing the Walker A, Walker B and the ABC signature motifs characteristic of all classical ABC transporters. In principle, CblD might be a B_{12}-binding protein which accepts the cofactor from CblC and delivers it to the client enzymes, methionine synthase and methylmalonyl-Co Amutase. In support of this proposal is the presence of a signature DxHxxG-39/40–gxSxLxxxx–17/18-xxxxGGx B_{12}-binding sequence [17], albeit incomplete. Alternatively, CblD might

[2]CblD is also referred to as MMADHC (for methylmalonic aciduria type D with homocystinuria) [9]. Since this nomenclature does not aptly describe the heterogeneity in this patient group, i.e. not all individuals exhibit combined methylmalonic aciduria and homocystinuria, we use CblD to refer to the gene product of the *cbl*D locus.

NIH-PA Author Manuscript

NIH-PA Author Manuscript

NIH-PA Author Manuscript

influence the activity of CblC either at the level of B_{12} processing (i.e. its dealkylation and decyanation activities) or at the level of its interactions with downstream client proteins facilitating transfer of B_{12} from the CblC donor to the cytoplasmic and mitochondrial acceptors. Finally, CblD could be involved further downstream i.e., in docking of the cofactor to the target enzymes, methionine synthase and methylmalonyl-CoA mutase, respectively.

In this study, we have purified four forms of recombinant human CblD with varying N-terminal start sites at residues 1, 12, 62 and 116, respectively. We demonstrate that CblD does not bind B_{12} nor exhibits ATPase activity. All four CblD variants form complexes with and exhibit selectivity for the B_{12} cofactor bound form of CblC compared to apo-CblC. We propose that CblD might function as an adapter for complexation of CblC·cob(II)alamin to acceptor proteins: methionine synthase in the cytoplasm and either adenosyltransferase or a transporter in the mitochondrion (Fig. 1). In support of this model, we demonstrate that fibroblasts from *cblD* patients dealkylate [^{57}Co]-MeCbl but that the subsequent partitioning of the cobalamin product to MeCbl versus AdoCbl is affected by the location of the mutation in CblD. Mutations near the N- and C-termini of the protein diminish AdoCbl and MeCbl synthesis, respectively, while mutations in the middle affect both pathways. Hence, while CblD is not required for the activity of CblC per se, it affects partitioning of the processed cobalamin product of CblC into the cytoplasmic and mitochondrial pathways.

1. Materials and methods

1.1. Materials

All chemicals were purchased from Sigma unless otherwise stated. [^{57}Co]-MeCbl was synthesized by the reaction of [^{57}Co]-cob(I) alamin with methyl iodide (Sigma) under dim red light and anaerobic conditions as described previously [18]. Pfu polymerase, dNTPs and restriction enzymes were from NEB. Advanced DMEM and Dulbecco's phosphate buffered saline (PBS) were purchased from Gibco.

1.2. Cloning of CbD variants

The cDNA encoding CblD in the pcDNA3.2/V5/GW/D-TOPO vector was generously provided by Dr. Brian Fowler (University Children's Hospital, Basel). Four start sites (at positions 1, 12, 62 and 116) were used to clone the gene into the pET-28b(+) vector (Novagen) using the *Nco*I/*Xho*I and *Nde*I/*Xho*I restriction enzyme sites to generate the C- and N-terminal 6×His-tagged constructs, respectively. Oligonucleotides containing the first and the last 24 bases of *cblD* gene with the restriction sites at their 5′-end, were used as primers as described below. The underlined bases correspond to the *Nde*I and *Xho*I restriction sites that were designed into the forward and reverse primer sequences, respectively.

Forward M1: 5′-CATATGGCCAATGTGCTTTGTAACAGAGCC-3′,

Forward S12: 5′-CATATGGTTTCCTATCTCCCAGGATTTTGC-3′,

Forward M62: 5′-CATATGGGACCCTTTGGACCTCAAGATCAG-3′,

Forward M116: 5′-CATATGGCACAATATGTGAATGAATTTCAG-3′,

Reverse: 5′-CTCGAGTTAATTTCCACTTAATTTCTTCAT-3′.

1.3. Expression and purification of CblD proteins

The *Escherichia coli* strain BL21(DE3) was freshly transformed with the desired plasmid constructs and grown in Luria–Bertani (LB) medium containing kanamycin (50 μg/ml) at 37 °C, induced with 0.25 mM isopropyl β-D-1-thiogalactopyranoside (IPTG) (at $A_{600\ nm}$ = 0.5–

NIH-PA Author Manuscript

NIH-PA Author Manuscript

NIH-PA Author Manuscript

0.7), and then grown overnight (~12 h) at 20 °C. The cells were harvested by centrifugation and the cell pellet was stored at −80 °C until further use.

Recombinant CblD was prepared by resuspending the cell pellets in lysis/binding buffer (50 mM Tris, pH 8.0, 300 mM KCl, 15 mM imidazole (Buffer A)) supplemented with 10 mM β-mercaptoethanol, lysozyme (0.2 mg/ml) and one tablet of Complete-EDTA protease inhibitor (Roche). Cells were disrupted by sonication and centrifuged at 20,000 × *g* for 1 h and the supernatant was applied to a 15 ml nickel–nitrilotriacetic acid column (Qiagen). The column was washed with 50 mM Tris, pH 8.0, 300 mM KCl, 50 mM imidazole until the flow-through was protein-free and recombinant CblD was eluted with a 50–400 mM imidazole gradient. The fractions of interest identified by SDS-PAGE were pooled, concentrated and the buffer was exchanged with 100 mM Hepes, pH 7.0, 150 mM KCl, 10% glycerol (Buffer B).

1.4. Size exclusion chromatography

The oligomeric state of the CblD variants was determined by loading 1–2.5 mg protein on a Superdex 200 column (1.6 × 80 cm) in Buffer B at a flow rate of 0.5 ml/min. The column was calibrated using gel filtration standards from Bio-Rad.

1.5. Binding of B_{12} derivatives and ATP to CblD

Binding of MeCbl, AdoCbl and HOCbl to CblD was examined by isothermal titration calorimetry (ITC) and fluorescence or UV–visible spectroscopy. Fluorescence measurements were made on an RF-5301 PC Shimadzu spectrofluorimeter at 280 nm excitation wavelength (slit width, 3 μm) and the emission was observed between 300 and 380 nm (slit width, 3 μm). The experiments were performed at 20 °C in a fluorescence quartz cuvette and successive aliquots (1–2 μl) of B_{12} stock solution (5–15 mM) were added to a 0.5 μM CblD solution in Buffer B. Similarly, binding of ATP to CblD was determined using 10–100 mM stock solutions. In the ITC experiments, CblD (10–40 μm) was titrated with twenty four 12-μl aliquots of a 200–800 μm solution of B_{12} or ATP in Buffer B at 10.0 ± 0.1 °C. The calorimetric signals were integrated, and the data were analyzed with Microcal ORIGIN software.

1.6. Effect of CblD on B_{12} binding to CblC

The binding of CNCbl and MeCbl to CblC in the presence or absence of CblD was monitored by ITC as previously described [19]. CblC and CblD (5–40 μM) were added at a 1:1 ratio and titrated with 100–800 μM of B_{12}.

1.7. ATPase activity of CblD

The ATPase activity of CblD forms was carried out using a continuous assay coupled to pyruvate kinase/lactate dehydrogenase [20]. The reactions were carried out at 22 °C in 50 mM Tris–Cl, pH 8.0, 5 mM $MgCl_2$. The reaction mixtures were supplemented with 200 μM NADH, 3 mM phosphoenolpyruvate, 2–20 U pyruvate kinase, 2–20 U lactate dehydrogenase and 1 mMATP and incubated for 5min at 22 °C prior to addition of the CblD protein. ATP hydrolysis was followed by measuring the decrease in absorbance at 340 nm.

1.8. Effect of CblD on the catalytic activities of CblC

Anaerobic decyanation and aerobic dealkylation reactions catalyzed by CblC were monitored as described previously [19,21] with the exception that CblD was added to the reaction mixture at a 1:1 ratio with CblC.

NIH-PA Author Manuscript

NIH-PA Author Manuscript

NIH-PA Author Manuscript

1.9. Analysis of CblC:CblD complexes

Complex formation between CblD and CblC was tested by incubating 10–15 μg of CblC with an equal amount of CblD in the presence or absence of 100 μm MeCbl, CNCbl or HOCbl and 1 mM GSH at 20 °C in 100 mM Hepes, pH 8, 150 mM KCl, 10% glycerol. After 30 min, the mixtures were analyzed by polyacrylamide gel electrophoresis under nondenaturing conditions on a 4–20% gradient gel (Bio-Rad) over ~2 h at 4 °C.

1.10. Limited proteolysis of CblD proteins

CblD protein variants (15 μg) were incubated with trypsin (2% w/w) at room temperature for 10 min. The limited proteolysis reactions were stopped by addition of 1 μl TLCK (10% w/v). The digested proteins were then separated by electrophoresis on a 12% SDS-PAGE gel.

1.11. Cell culture and [^{57}Co]-MeCbl metabolic labeling

Normal and *cblD* mutant fibroblasts were grown in Advanced DMEM (Gibco) supplemented with 10% fetal bovine serum (FBS). Normal human skin fibroblast (HFF) was kindly provided by the Cell Culture Core of the Lerner Research Institute, Cleveland Clinic. The two normal cell lines used in the present study were generated from discarded tissue from circumcised donors of 1 and 3 months of age, respectively as described previously [18]. Human foreskin tissue was obtained for establishment of control skin fibroblast cultures after informed consent was received. The Institutional Review Board of the Cleveland Clinic approved the protocol. David Rosenblatt (McGill University) kindly provided human *cblD* mutant skin fibroblasts from patients with either isolated or combined homocystinuria and methylmalonic aciduria (WG2024, WG3280, WG3583 and WG3745) obtained as described previously [9,22]. The Royal Victoria Hospital Research Ethics Board (Montréal, Canada) approved the research protocol for procurement of patient skin biopsies.

For metabolic labeling experiments, cells were split at a ratio of 1:2 and [^{57}Co]-MeCbl was added to achieve a final concentration of 0.125 nM (specific activity: 379 mCi/mg MeCbl). After 48 h, cells were harvested, total cobalamins extracted with 80% aqueous ethanol and the intracellular cobalamin profile determined as described previously [18]. The cell cultures were protected from light at all times to prevent photolysis of the alkylcobalamins.

1.12. Determination of homocysteine and methylmalonic acid in culture medium

Cells were cultured as described and at the end point of the experiment, the culture medium was collected, centrifuged at 1000 rpm for 10 min (to remove dead cells), filtered using a 0.22 mm filter (Millipore) and stored at 4 °C until further use. Total homocysteine in culture medium was determined using monobromobimane and HPLC with fluorescence detection [23]. The concentration of methylmalonic acid in conditioned culture medium was determined by gas chromatography and mass spectrometry in the Department of Clinical Pathology, Cleveland Clinic by a method modified from Hoffmann et al. [24]. Briefly, methylmalonic acid was extracted from conditioned culture medium along with tri-deuterated methylmalonic acid (internal standard, MSD Isotopes) using Bond-Elute SAX solid phase extraction columns (Varian). The extracted acid was then derivatized with cyclohexanol to form a dicyclohexyl ester. The derivatized samples were resolved by gas chromatography and detected by mass spectrometry using selective ion monitoring. Values were normalized to intracellular protein concentration determined by the bicinchoninic acid assay (Thermo Scientific) using bovine serum albumin as a standard.

NIH-PA Author Manuscript

NIH-PA Author Manuscript

NIH-PA Author Manuscript

2. Results

2.1. Purification of recombinant CblD variants

Based on sequence analysis using MitoProt II and PSORT II, the CblD protein sequence is predicted to include a putative mitochondrial targeting sequence that spans residues 1–12 at the N-terminus to give the CblD ΔN11 variant [9]. Furthermore, two internal Met62 and Met116 codons have been shown to function as alternative translation initiation sites giving rise to ΔN61 and ΔN115-CblD variants [16]. We purified the recombinant full-length, ΔN11-, ΔN61- and ΔN115-CblD proteins to >95% homogeneity (Fig. 2). Since we found that the C-terminal His-tagged constructs were considerably less stable than the corresponding N-terminal tagged ones, only the latter were further characterized in this study. CblD as isolated, is devoid of a visible absorption spectrum suggesting the absence of a bound cofactor. These wild-type CblD variants were also devoid of a metal cofactor as assessed by plasma emission spectroscopy [25] at the Chemical Analysis Laboratory, University of Georgia, Athens (not shown). Size exclusion chromatography revealed that CblD is a monomer with estimated molecular masses of 35 kDa, 33.5 kDa, 28.5 kDa and 22.4 kDa, respectively for the full-length and the three N-terminal truncated variants. All CblD variants displayed a tendency to form high molecular weight aggregates.

2.2. Binding of B_{12} by CblD

Despite the presence of a weakly conserved B_{12}-binding motif in CblD, we found no evidence for binding of MeCbl, AdoCbl or HOCbl to this protein as determined by fluorescence, ITC and UV–visible spectroscopic studies. To test whether the 6×His-tag on CblD could be interfering with B_{12} binding, we cleaved it from the purified recombinant protein using thrombin. However, the absence of a His-tag did not promote B_{12} binding to CblD under the conditions employed in our assay.

2.3. CblD-catalyzed ATP hydrolysis

The putative ATPase activity of CblD was assessed using a previously described continuous assay [20]. Despite the sequence similarity with the ATPase component of the *Salmonella enterica* ABC transporter, CblD does not hydrolyze ATP.

2.4. Effect of CblD on B_{12} binding and processing by CblC

The presence of either full-length or ΔN11 CblD had essentially no effect on the affinity of CblC for CNCbl (K_d = 11.4 ± 1.6 μM versus 14.2 ± 2.1 μM) or MeCbl (K_d = 0.22 ± 0.02 μM versus 0.19 ± 0.02 μM). Similarly, the CblC-catalyzed rates for the reductive decyanation of CNCbl and the dealkylation of MeCbl by glutathione reported previously [19,21] were comparable in the presence or absence of full-length, ΔN11 or ΔN115 CblD (not shown).

2.5. Complex formation between CblD and CblC

Since CblD does not appear to influence B_{12} binding or the B_{12} processing activities of CblC, we next looked for evidence for interactions between these two proteins. In the absence of B_{12}, CblC behaves like a higher order oligomer that barely migrates into the gel (Fig. 3A, lane 11). Addition of CNCbl in the presence or absence of glutathione induced an electrophoretic shift in CblC which ran with an apparent molecular mass of ~250 kDa (Fig. 3A, lanes 12–13). The presence of AdoCbl and/or glutathione had no effect on the CblD electrophoretic pattern that migrated with a molecular mass of ~50 kDa (Fig. 3A, lanes 14–16), although the protein behaves as a monomer with a predicted molecular size of ~35 kDa by size exclusion chromatography (not shown). When CblC and CblD were pre-incubated, a new band was visualized but only in the presence of B_{12} (compare lane 6 with lanes 2–5).

NIH-PA Author Manuscript

NIH-PA Author Manuscript

NIH-PA Author Manuscript

Addition of glutathione versus dithiothreitol to the CblD:CblC·B_{12} mixture enhanced complex formation (compare lanes 2–5 versus 7–10), in particular the complexes formed in the presence of MeCbl and AdoCbl. Since the protein samples were incubated for 30 min prior to being loaded on the native gel, CblC would have catalyzed the dealkylation of MeCbl, and to a lesser extent, of AdoCbl, by GSH leading to HOCbl formation (via air oxidation of the product, cob(I)alamin). These results suggest that when an alkylcobalamin substrate is bound to CblC, it inhibits complex formation with CblD. Instead, CblD preferentially interacts with the product complex, i.e. after CblC-catalyzed dealkylation has occurred. Similarly, the CblC:CblD complex is seen in the presence of glutathione and HOCbl (Fig. 3A, lane 5), a condition that simulates the product complexes formed in lanes 2 and 3 in the presence of glutathione and AdoCbl and MeCbl, respectively. Separation of the excised band representing the CblD·CblC complex on a denaturing polyacrylamide gel revealed the presence of two bands corresponding to full-length CblC (33 kDa) and full-length CblD (~35 kDa) respectively in approximately 1:1 stoichiometry (Fig. 3B). Although interactions between CblC and CblD were assessed using the respective His-tagged proteins, an influence of the tags on protein–protein interaction appears unlikely since the interaction was specific for the presence of glutathione and a cobalamin derivative (e.g. HOCbl, MeCbl or AdoCbl).

Qualitatively similar results for complex formation with CblC were obtained with CblD-ΔN11, -ΔN61 and -ΔN115 (Fig. 4A, lanes 7, 5 and 3). These results demonstrate that the N-terminal 115 residues in CblD are dispensable for its interaction with CblC. The shorter variant of CblC, lacking the C-terminal residues from 246 to 282, which we have determined as the predominant form of CblC in the murine tissue extracts [26], also formed a complex with CblD indicating that these residues are dispensable for protein–protein interaction (data not shown).

2.6. Limited proteolysis of CblD proteins

Treatment of the CblD variants with trypsin revealed the presence of a core that was common to the ΔN11 and ΔN61 variants and just slightly smaller for the ΔN115 variant (Fig. 4B). Stabilization of a similar sized fragment in the N-terminal deletion variants is consistent with the existence of two domains in CblD of which the C-terminal domain is sufficient for the interaction with CblC. Preincubation of CblD-ΔN61 for 30 min with 1 mM concentrations of the following ligands: ATP, ADP, HOCbl, flavin adenine dinucleotide, NADH and NADPH, did not affect its limited proteolysis profile (not shown).

2.7. Growth and morphology of the cblD cell lines

The mutations in each of the *cblD* fibroblast cell lines are described in Table 1. Although none of the cell lines displayed gross impairments, slower growth was observed for the *cblD* lines compared to normal fibroblasts when they were seeded at low density (<40%). With the exception of the WG3583 cell line, the remaining *cblD* fibroblast lines presented an altered morphology, with slightly enlarged cellular body size and a disrupted fibroblast growth pattern, as evidenced by phase-contrast microscopy (Fig. 5).

2.8. Production of homocysteine and methylmalonic acid

Based on the known impairment of AdoCbl and/or MeCbl assimilation in *cblD* cell lines, we expected that media from these cell cultures would have higher levels of methylmalonic acid and/or homocysteine compared to normal fibroblasts. Table 2 shows the levels of homocysteine and methylmalonic acid in the culture medium after 5 days. With the exception of cell line WG3280 (a patient with isolated methylmalonic aciduria), all *cblD* cell lines accumulated substantially higher (>2-fold) extracellular homocysteine compared to

NIH-PA Author Manuscript

NIH-PA Author Manuscript

NIH-PA Author Manuscript

normal fibroblasts. Normal values for homocysteine and methylmalonic acid in cultured human fibroblasts are given in this study and elsewhere [27-29].

The levels of methylmalonic acid are clearly elevated 10–25-fold in fibroblast cultures from cells from patients with isolated or combined methylmalonic aciduria versus either homocystinuria alone or unaffected controls (Table 2). The extracellular methylmalonic acid was highest in the WG3280 cell culture (from a patient with isolated methylmalonic aciduria). Together, these data indicate that the *cblD* cell lines selected for the present study represent a good model for studying functional cobalamin deficiency representing both the isolated and combined phenotypes.

2.9. CblC-dependent dealkylation of MeCbl is not impaired in cblD cell lines

We have previously demonstrated that cell lines with defects in the *cblC* locus are unable to dealkylate alkylcobalamins, which are needed for subsequent partitioning into the AdoCbl and MeCbl assimilation pathways [18,19]. To test the cellular relevance of our observation that CblD does not influence the dealkylation activity of CblC in vitro, metabolic labeling studies were performed. For this, incorporation of exogenously supplied [^{57}Co]-MeCbl into AdoCbl and MeCbl was examined (Table 3). The major intracellular cobalamin derivative observed in all *cblD* cell lines was [^{57}Co]-HOCbl indicating that the newly internalized [^{57}Co]-MeCbl had been dealkylated by CblC and the product was subsequently oxidized to HOCbl.

2.10. Redistribution of cofactor pools in cblD cell lines

Variable total intracellular retention of [^{57}Co]-cobalamin was observed in the different cells lines. The WG2024 and WG3745 lines showed values that were similar to the control line, HFF, while significantly higher retention was seen in WG3280 and lower accumulation in the WG3583 line (Table 3). The relative proportions of the MeCbl and AdoCbl pools in the control cell line were typical of the relative abundance reported previously for these two cofactors [15,18,30]. All *cblD* cell lines displayed altered cofactor distribution (Table 3 and Fig. 6). The presence of [^{57}Co]-HOCbl in *cblD* cell lines suggested impairments downstream of CblC in the trafficking pathway.

The distribution of [^{57}Co]-cobalamin in the *cblD* line with the isolated methylmalonic aciduria (WG3280) or homocystinuria (WG3745) phenotype was interesting. Very low incorporation of radiolabel into the AdoCbl pool was observed in WG3280, consistent with impairment in the mitochondrial-specific pathway. However, a proportional increase in radioactivity associated with the MeCbl pool was seen, suggesting that the inability to direct HOCbl into the AdoCbl pathway led to an increased flux into the MeCbl branch (Fig. 6).

In contrast, very low levels of [^{57}Co]-MeCbl were observed in the WG3745 cell line, consistent with an impairment in the cytoplasmic-specific pathway. Very high levels of [^{57}Co]-AdoCbl (76% of the total [^{57}Co]-cobalamin pool) and a proportionately lower level of [^{57}Co]-HOCbl was seen in WG3745 compared to the normal fibroblast cell line (Fig. 6). Together, these results suggest that the failure of the CblD protein to direct newly processed cobalamin into the biosynthesis of one of the cofactors leads to an overproduction of the other cofactor.

The intracellular pattern of distribution of radiolabeled cobalamins in the two cell lines with combinedmethylmalonic aciduria and homocystinuria, WG2024 and WG3583, was similar. In both lines, the MeCbl pool was more compromised than the AdoCbl pool and this was paralleled by an increase in the proportion of HOCbl.

NIH-PA Author Manuscript

NIH-PA Author Manuscript

NIH-PA Author Manuscript

3. Discussion

Delivery of cobalamin from circulation to its intracellular clients requires an elaborate system of transporters, escorts and B_{12} processing enzymes, which results in assimilation of the cofactor into its biologically active forms, MeCbl and AdoCbl, which are utilized by methionine synthase and methylmalonyl-CoA mutase, respectively (Fig.1) [1,2]. MeCbl is the predominant form of the cofactor in human plasma [31], and following its entry into cells, it must be dealkylated by the action of CblC to be subsequently partitioned to meet cellular demands for the MeCbl and AdoCbl cofactor forms [19]. While the role of CblD is expected to be downstream of CblC, identification of the *cblD* gene did not provide obvious insights into the role of the encoded protein. The low sequence homology between residues 78 and 168 of CblD and the ATPase component of a bacterial ABC transporter, suggests that it might hydrolyze ATP [9]. On the other hand, based on the presence of a partially conserved canonical B_{12} binding motif at the N-terminus of the protein, it was proposed that CblD might be involved in binding the cofactor [9].

Full-length CblD was shown to interact with CblC in a bacterial two hybrid study and by surface plasmon resonance (SPR) [32], although the stoichiometry and ligand dependence of complex formation was not assessed since the CblD was only partially purified. While our study was in progress, the stoichiometric interaction between purified CblD-ΔN12 and CblD-ΔN61 and full-length CblC by SPR was reported [33]. In this study, we have used a combination of biochemical and cell biological approaches to elucidate complexation of four CblD variants with a full-length and a truncated variant of CblC and have evaluated the consequences of CblD deficiency on MeCbl and AdoCbl processing.

We have expressed and purified four recombinant CblD variants (Fig. 2) and demonstrate that these monomeric proteins as isolated, are devoid of metal and organic cofactors with detectable absorption spectra. Furthermore, CblD does not appear to bind B_{12} or to hydrolyze ATP. Based on these results, we propose that CblD functions instead as an adapter protein. A traffic junction where CblD might be involved is the transfer of the B_{12} cargo from CblC to acceptors in the MeCbl and AdoCbl branches as shown in Fig. 1. This model is supported by the enhanced interaction between CblC and CblD observed in the presence of glutathione and HOCbl (Fig. 3A), the processed and oxidized product of the CblC-catalyzed dealkylation of alkylcobalamins. A weak complex is also observed in the presence of CNCbl.

While the shorter ΔN61 and ΔN115 variants are predicted to be physiologically relevant only when mutations in *cblD* lead to isolated methylmalonic aciduria, their ability to retain complex formation with CblC indicates that the first 115 residues are dispensable for protein–protein interaction. This is consistent with results from a phage display analysis that identified five short peptides between residues 142 and 290 in CblD as being potentially important for binding to CblC [32]. Similarly, the last 37 residues in CblC present in the full-length form of the protein shown to be expressed in human cell lines [33] but not in murine tissue [26] is not needed for complexation with CblD. It is not known how B_{12} is delivered to the mitochondrion to support the AdoCbl branch of the pathway. A possible role for the N-terminal domain of CblD in the transfer of the B_{12} from CblC to a mitochondrial transporter as depicted in Fig. 1 can be considered.

The presence of a weak leader sequence at the N-terminus predicts that CblD also resides in the mitochondrion. While localization in the mitochondrial compartment has not been shown, transfection of a CblD construct containing the strong aldehyde dehydrogenase-2 mitochondrial leader sequence has been shown to improve the levels of AdoCbl in a *cblD* cell line with a combined MMA/homocystinuria defect [16]. Based on mutational analysis

NIH-PA Author Manuscript

NIH-PA Author Manuscript

NIH-PA Author Manuscript

of CblD, the N-terminal domain is expected to be involved in targeting B_{12} bound to CblC to the mitochondrial pathway while the C-terminal domain could deliver it to the cytoplasmic acceptor, presumably methionine synthase [9]. Interestingly, the presence of CblC in the mitochondrion has been reported in a mitochondrial proteomic study [34]. Furthermore, *cblC* cell lines reportedly exhibit elevated reactive oxygen species levels and a higher propensity for undergoing apoptosis [35], suggestive of a mitochondrial connection. However, the presence of CblC in the mitochondrion has not been independently verified by localization or other studies and needs to be addressed before its involvement in mitochondrial delivery of the cofactor to the next protein in the trafficking pathway, adenosyltransferase, can be assessed.

The *cblD* group is among the rarest of cobalamin disorders and also the most complex in the heterogeneity of clinical presentations that range from isolated to combined deficiency in the MeCbl and AdoCbl branches of the trafficking pathway [15]. Cellular analysis of the fate of [^{57}Co]-MeCbl in fibroblasts from *cblD* patients with isolated or combined B_{12} deficiency provide compelling evidence for the role of CblD being downstream of CblC. Our study shows that while MeCbl is dealkylated (a function of CblC) in *cblD* cell lines, the partitioning of the resulting cofactor product between the cytosolic and mitochondrial compartments is significantly impaired. A previous report on three of the four *cblD* cell lines used in this study (WG3280, WG3583 and WG3745) also revealed changes in the proportion of AdoCbl versus MeCbl when cells were fed [^{57}Co]- CNCbl [22]. These results further support our conclusion that the function of CblD is downstream of CblC in the cobalamin trafficking pathway since we have shown that CblC decyanates CNCbl [21].

Perturbed intracellular cobalamin distribution in *cblD* cell lines points to a role for CblD in guiding cofactor traffic between competing pathways. In the WG3280 cell line, one allele has a p.L20fsX21 mutation, i.e. a frame shift at L20 leads to termination at codon 21 (Table 1). Hence, the translation product of this allele initiating at codon 1would lead to a truncated CblD product. On the other hand, internal initiation at codon 62 would give rise to a shorter CblD-NΔ61 product. The other allele has a frame shift mutation leading to truncation at codon 162 (pT152fsX162), which is expected to impair both the mitochondrial and cytoplasmic forms of CblD. In this cell line, there is both a large redirection of the intracellular cobalamin pool to MeCbl synthesis at the expense of AdoCbl synthesis, and surprisingly, a net increase in the intracellular B_{12} pool size (Table 3). Curiously, the total radioactivity in AdoCbl is greater than in the control cell line, but the MeCbl:AdoCbl ratio is 6.4 in WG3280 versus 1.8 in the control.

One mechanism for the increase in total B_{12} could be via translational up-regulation of methionine synthase, which occurs via a B_{12}-responsive IRES element that is sensitive to MeCbl but not AdoCbl [36]. Increased synthesis of methionine synthase would lead to increased production of MeCbl, which occurs in situ on the enzyme and to which it remains tightly bound. Methionine synthase, in turn, is stabilized by binding of B_{12} [37].

Isolated deficiency of methionine synthase occurs in the WG3745 line, which is homozygous for the D246G mutation in CblD. In this cell line, the total B_{12} levels are approximately in the same range as in control, but a very high proportion (76%) is tied up as AdoCbl while MeCbl represents only 6% of the total pool and the MeCbl:AdoCbl ratio is 0.09. In contrast, in the control cell line, AdoCbl and MeCbl represent 23% and 42% of the total pool size, respectively (Table 3). The cofactor distribution is indicative of greater cobalamin availability for the mitochondrial assimilation pathway when a mutation selectively impairs the cytoplasmic CblD function. It also suggests that under normal conditions, partitioning of cobalamin to methionine synthase and to MeCbl synthesis may be a priority. This is supported by the observation that a significant proportion of

NIH-PA Author Manuscript

NIH-PA Author Manuscript

NIH-PA Author Manuscript

methylmalonyl-CoA mutase exists in the apo-form [38] whereas methionine synthase is largely present in the holoenzyme form [39].

The combined phenotype of the *cblD* disease leads to a milder defect in the biosynthesis of AdoCbl and MeCbl compared to the outcome in the isolated cases (Table 3). The mechanistic basis of this finding is presently unknown. While all the *cblD* fibroblasts show perturbations in cofactor partitioning to MeCbl versus AdoCbl relative to the control cell line, net diminution in the cofactor pool is consistently observed only for MeCbl (i.e. in cell lines from patients with isolated or combined homocystinuria). This is consistent with our model that CblD plays a role in cofactor loading on to methionine synthase, the site of MeCbl synthesis (Fig. 1). In contrast, the AdoCbl pool size is not a predictor of associated methylmalonic aciduria. Indeed, in two cell lines from patients with *cblD*-associated methylmalonic aciduria, WG2024 and WG3280, AdoCbl levels are equal to or higher than in the control cell line (Table 3). This suggests that loading of methylmalonyl-CoA mutase with AdoCbl is impacted by mutations in the mitochondrial CblD but AdoCbl synthesis per se is not. Based on this observation, we tentatively propose that CblD functions in the transfer complex between adenosyltransferase (CblB) and methylmalonyl-CoA mutase (Mut), which presumably exists in complex with its Gprotein chaperone (CblA) in the cell (Fig. 1). In the bacterial orthologs of these mitochondrial proteins, adenosyltransferase synthesizes and then directly transfer AdoCbl to the mutase·CblA complex [40-42]. In bacteria, orthologs of CblD and CblC are not found; hence the details of the cofactor docking mechanisms are likely to be different from the mammalian pathway.

In summary, our study maps the involvement of CblD downstream of CblC in the cobalamin trafficking pathway and reveals that the C-terminal domain is sufficient for interaction with CblC. Since CblD does not appear to bind B_{12} directly, at least under the conditions tested in this study, we suggest that CblD might play a role in delivery of the cofactor from CblC to methionine synthase in the cytoplasm and possibly, to a mitochondrial acceptor. The mitochondrially-directed CblD might be similarly involved in cofactor loading onto adenosyltransferase (CblB), which synthesizes AdoCbl and/or further downstream, i.e. cofactor docking to methylmalonyl-CoA mutase.

Acknowledgments

We acknowledge Austin Stevens for his assistance with the initial characterization of the CblD-ΔN115 variant. This work utilized the Morphology and Image Analysis Cores of the Michigan Diabetes Research and Training Center funded by NIH5P60 DK20572 from the National Institute of Diabetes & Digestive & Kidney Diseases.

References

1. Banerjee R. B_{12} trafficking in mammals: a case for coenzyme escort service. ACS Chem Biol. 2006; 1:149–159. [PubMed: 17163662]
2. Banerjee R, Gherasim C, Padovani D. The tinker, tailor, soldier in intracellular B_{12} trafficking. Curr Opin Chem Biol. 2009; 13:477–484.
3. Gravel RA, Mahoney MJ, Ruddle FH, Rosenberg LE. Genetic complementation in heterokaryons of human fibroblasts defective in cobalamin metabolism. Proc Natl Acad Sci U S A. 1975; 72:3181–3185. [PubMed: 1059104]
4. Willard HF, Mellman IS, Rosenberg LE. Genetic complementation among inherited deficiencies of methylmalonyl-CoA mutase activity: evidence for a new class of human cobalamin mutant. Am J Hum Genet. 1978; 30:1–13. [PubMed: 23678]
5. Shevell MI, Rosenblatt DS. The neurology of cobalamin. Can J Neurol Sci. 1992; 19:472–486. [PubMed: 1423045]
6. Coelho D, Kim JC, Miousse IR, Fung S, du Moulin M, Buers I, Suormala T, Burda P, Frapolli M, Stucki M, Nurnberg P, Thiele H, Robenek H, Hohne W, Longo N, Pasquali M, Mengel E, Watkins

NIH-PA Author Manuscript

NIH-PA Author Manuscript

NIH-PA Author Manuscript

D, Shoubridge EA, Majewski J, Rosenblatt DS, Fowler B, Rutsch F, Baumgartner MR. Mutations in ABCD4 cause a new inborn error of vitamin B12 metabolism. Nat Genet. 2012; 44:1152–1155. [PubMed: 22922874]

7. Rutsch F, Gailus S, Miousse IR, Suormala T, Sagne C, Toliat MR, Nurnberg G, Wittkampf T, Buers I, Sharifi A, Stucki M, Becker C, Baumgartner M, Robenek H, Marquardt T, Hohne W, Gasnier B, Rosenblatt DS, Fowler B, Nurnberg P. Identification of a putative lysosomal cobalamin exporter altered in the cblF defect of vitamin B_{12} metabolism. Nat Genet. 2009; 41:234–239. [PubMed: 19136951]
8. Lerner-Ellis JP, Tirone JC, Pawelek PD, Dore C, Atkinson JL, Watkins D, Morel CF, Fujiwara TM, Moras E, Hosack AR, Dunbar GV, Antonicka H, Forgetta V, Dobson CM, Leclerc D, Gravel RA, Shoubridge EA, Coulton JW, Lepage P, Rommens JM, Morgan K, Rosenblatt DS. Identification of the gene responsible for methylmalonic aciduria and homocystinuria, *cblC* type. Nat Genet. 2006; 38:93–100. [PubMed: 16311595]
9. Coelho D, Suormala T, Stucki M, Lerner-Ellis JP, Rosenblatt DS, Newbold RF, Baumgartner MR, Fowler B. Gene identification for the cblD defect of vitamin B_{12} metabolism. N Engl J Med. 2008; 358:1454–1464. [PubMed: 18385497]
10. Dobson CM, Wai T, Leclerc D, Kadir H, Narang M, Lerner-Ellis JP, Hudson TJ, Rosenblatt DS, Gravel RA. Identification of the gene responsible for the *cblB* complementation group of vitamin B_{12}-dependent methylmalonic aciduria. Hum Mol Genet. 2002; 11:3361–3369. [PubMed: 12471062]
11. Dobson CM, Wai T, Leclerc D, Wilson A, Wu X, Dore C, Hudson T, Rosenblatt DS, Gravel RA. Identification of the gene responsible for the *cblA* complementation group of vitamin B_{12}-responsive methylmalonic acidemia based on analysis of prokaryotic gene arrangements. Proc Natl Acad Sci U S A. 2002; 99:15554–15559. [PubMed: 12438653]
12. Leal NA, Park SD, Kima PE, Bobik TA. Identification of the human and bovine ATP: cob(I)alamin adenosyltransferase cDNAs based on complementation of a bacterial mutant. J Biol Chem. 2003; 278:9227–9234. [PubMed: 12514191]
13. Leclerc D, Wilson A, Dumas R, Gafuik C, Song D, Watkins D, Heng HHQ, Rommens JM, Scherer SW, Rosenblatt DS, Gravel RA. Cloning and mapping of a cDNA for methionine synthase reductase, a flavoprotein defective in patients with homocystinuria. Proc Natl Acad Sci U S A. 1998; 95:3059–3064. [PubMed: 9501215]
14. Hsu JM, Kawin B, Minor P, Mitchell JA. Vitamin B_{12} concentrations in human tissue. Nature. 1966; 210:1264–1265.
15. Suormala T, Baumgartner MR, Coelho D, Zavadakova P, Koich V, Koch HG, Berghauser M, Wraith JE, Burlina A, Sewell A, Herwig J, Fowler B. The c*blD* defect causes either isolated or combined deficiency of methylcobalamin and adenosylcobalamin synthesis. J Biol Chem. 2004:42742–42749. [PubMed: 15292234]
16. Stucki M, Coelho D, Suormala T, Burda P, Fowler B, Baumgartner MR. Molecular mechanisms leading to three different phenotypes in the cblD defect of intracellular cobalamin metabolism. Hum Mol Genet. 2012; 21:1410–1418. [PubMed: 22156578]
17. Drennan CL, Huang S, Drummond JT, Matthews RG, Ludwig ML. How a protein binds B12: a 3.0 A X-ray structure of B12-binding domains of methionine synthase. Science. 1994; 266:1669–1674. [PubMed: 7992050]
18. Hannibal L, Kim J, Brasch NE, Wang S, Rosenblatt D, Banerjee R, Jacobsen DW. Processing of alkylcobalamins in mammalian cells: a role for the MMACHC (*cblC*) gene product. Mol Genet Metab. 2009; 97:260–266. [PubMed: 19447654]
19. Kim J, Hannibal L, Gherasim C, Jacobsen DW, Banerjee R. A human vitamin B_{12} trafficking protein uses glutathione transferase activity for processing alkylcobalamins. J Biol Chem. 2009; 284:33418–33424. [PubMed: 19801555]
20. Nørby JG. Coupled assay of Na+, K+-ATPase activity. Methods Enzymol. 1988; 156:116–119. [PubMed: 2835597]
21. Kim J, Gherasim C, Banerjee R. Decyanation of vitamin B_{12} by a trafficking chaperone. Proc Natl Acad Sci U S A. 2008; 105:14551–14554. [PubMed: 18779575]

NIH-PA Author Manuscript

NIH-PA Author Manuscript

NIH-PA Author Manuscript

22. Miousse IR, Watkins D, Coelho D, Rupar T, Crombez EA, Vilain E, Bernstein JA, Cowan T, Lee-Messer C, Enns GM, Fowler B, Rosenblatt DS. Clinical and molecular heterogeneity in patients with the cblD inborn error of cobalamin metabolism. J Pediatr. 2009; 154:551–556. [PubMed: 19058814]
23. Jacobsen DW, Gatautis VJ, Green R, Robinson K, Savon SR, Secic M, Ji J, Otto JM, Taylor LM Jr. Rapid HPLC determination of total homocysteine and other thiols in serum and plasma: sex differences and correlation with cobalamin and folate concentrations in healthy subjects. Clin Chem. 1994; 40:873–881. [PubMed: 8087981]
24. Hoffmann G, Aramaki S, Blum-Hoffmann E, Nyhan WL, Sweetman L. Quantitative analysis for organic acids in biological samples: batch isolation followed by gas chromatographic-mass spectrometric analysis. Clin Chem. 1989; 35:587–595. [PubMed: 2702744]
25. Jones JBJ. Elemental analysis of soil extracts and plant tissue by plasma emission spectroscopy. Commun Soil Sci Plant Anal. 1977; 8:349–365.
26. Koutmos M, Gherasim C, Smith JL, Banerjee R. Structural basis of multifunctionality in a vitamin B_{12}-processing enzyme. J Biol Chem. 2011; 286:29780–29787. [PubMed: 21697092]
27. Kolhouse JF, Stabler SP, Allen RH. Identification and perturbation of mutant human fibroblasts based on measurements of methylmalonic acid and total homocysteine in the culture media. Arch Biochem Biophys. 1993; 303:355–360. [PubMed: 8099783]
28. Quadros EV, Lai SC, Nakayama Y, Sequeira JM, Hannibal L, Wang S, Jacobsen DW, Fedosov S, Wright E, Gallagher RC, Anastasio N, Watkins D, Rosenblatt DS. Positive newborn screen for methylmalonic aciduria identifies the first mutation in TCblR/CD320, the gene for cellular uptake of transcobalamin-bound vitamin B(12). Hum Mutat. 2010; 31:924–929. [PubMed: 20524213]
29. Hannibal L, DiBello PM, Yu M, Miller A, Wang S, Willard B, Rosenblatt DS, Jacobsen DW. The MMACHC proteome: hallmarks of functional cobalamin deficiency in humans. Mol Genet Metab. 2011; 103:226–239. [PubMed: 21497120]
30. Hannibal L, Axhemi A, Glushchenko AV, Moreira ES, Brasch NE, Jacobsen DW. Accurate assessment and identification of naturally occurring cellular cobalamins. Clin Chem Lab Med. 2008; 46:1739–1746. [PubMed: 18973458]
31. Chu RC, Begley JA, Colligan PD, Hall CA. The methylcobalamin metabolism of cultured human fibroblasts. Metabolism. 1993; 42:315–319. [PubMed: 8487649]
32. Plesa M, Kim J, Paquettea SG, Gagnona H, Ng-Thow-Hinga C, Gibbsb BF, Hancockb MA, Rosenblatt DS, Coultona JW. Interaction between MMACHC and MMADHC, two human proteins participating in intracellular vitamin B_{12} metabolism. Mol Genet Metab. 2011; 102:139–148. [PubMed: 21071249]
33. Deme JC, Miousse IR, Plesa M, Kim JC, Hancock MA, Mah W, Rosenblatt DS, Coulton JW. Structural features of recombinant MMADHC isoforms and their interactions with MMACHC, proteins of mammalian vitamin B_{12} metabolism. Mol Genet Metab. 2012; 107:352–362. [PubMed: 22832074]
34. Pagliarini DJ, Calvo SE, Chang B, Sheth SA, Vafai SB, Ong SE, Walford GA, Sugiana C, Boneh A, Chen WK, Hill DE, Vidal M, Evans JG, Thorburn DR, Carr SA, Mootha VK. A mitochondrial protein compendium elucidates complex I disease biology. Cell. 2008; 134:112–123. [PubMed: 18614015]
35. Richard E, Jorge-Finnigan A, Garcia-Villoria J, Merinero B, Desviat LR, Gort L, Briones P, Leal F, Perez-Cerda C, Ribes A, Ugarte M, Perez B. Genetic and cellular studies of oxidative stress in methylmalonic aciduria (MMA) cobalamin deficiency type C (cblC) with homocystinuria (MMACHC). Hum Mutat. 2009; 30:1558–1566. [PubMed: 19760748]
36. Oltean S, Banerjee R. A B_{12}-responsive IRES element in human methionine synthase. J Biol Chem. 2005; 280:32662–32668. [PubMed: 16051610]
37. Yamada K, Kawata T, Wada M, Isshiki T, Onoda J, Kawanishi T, Kunou A, Tadokoro T, Tobimatsu T, Maekawa A, Toraya T. Extremely low activity of methionine synthase in vitamin B_{12}-deficient rats may be related to effects on coenzyme stabilization rather than to changes in coenzyme induction. J Nutr. 2000; 130:1894–1900. [PubMed: 10917899]

NIH-PA Author Manuscript

NIH-PA Author Manuscript

NIH-PA Author Manuscript

38. Fenton WA, Hack AM, Willard HF, Gertler A, Rosenberg LE. Purification and properties of methylmalonyl coenzyme A mutase from human Liver. Arch Biochem Biophys. 1982; 214:815–823. [PubMed: 6124211]

39. Chen Z, Chakraborty S, Banerjee R. Demonstration that the mammalian methionine synthases are predominantly cobalamin-loaded. J Biol Chem. 1995; 270:19246–19249. [PubMed: 7642596]

40. Padovani D, Labunska T, Palfey BA, Ballou DP, Banerjee R. Adenosyltransferase tailors and delivers coenzyme B_{12}. Nat Chem Biol. 2008; 4:194–196. [PubMed: 18264093]

41. Padovani D, Banerjee R. A G-protein editor gates coenzyme B_{12} loading and is corrupted in methylmalonic aciduria. Proc Natl Acad Sci U S A. 2009; 106:21567–21572. [PubMed: 19955418]

42. Lofgren M, Banerjee R. Loss of allostery and coenzyme B_{12} delivery by a pathogenic mutation in adenosyltransferase. Biochemistry. 2011; 50:5790–5798. [PubMed: 21604717]

NIH-PA Author Manuscript

NIH-PA Author Manuscript

NIH-PA Author Manuscript

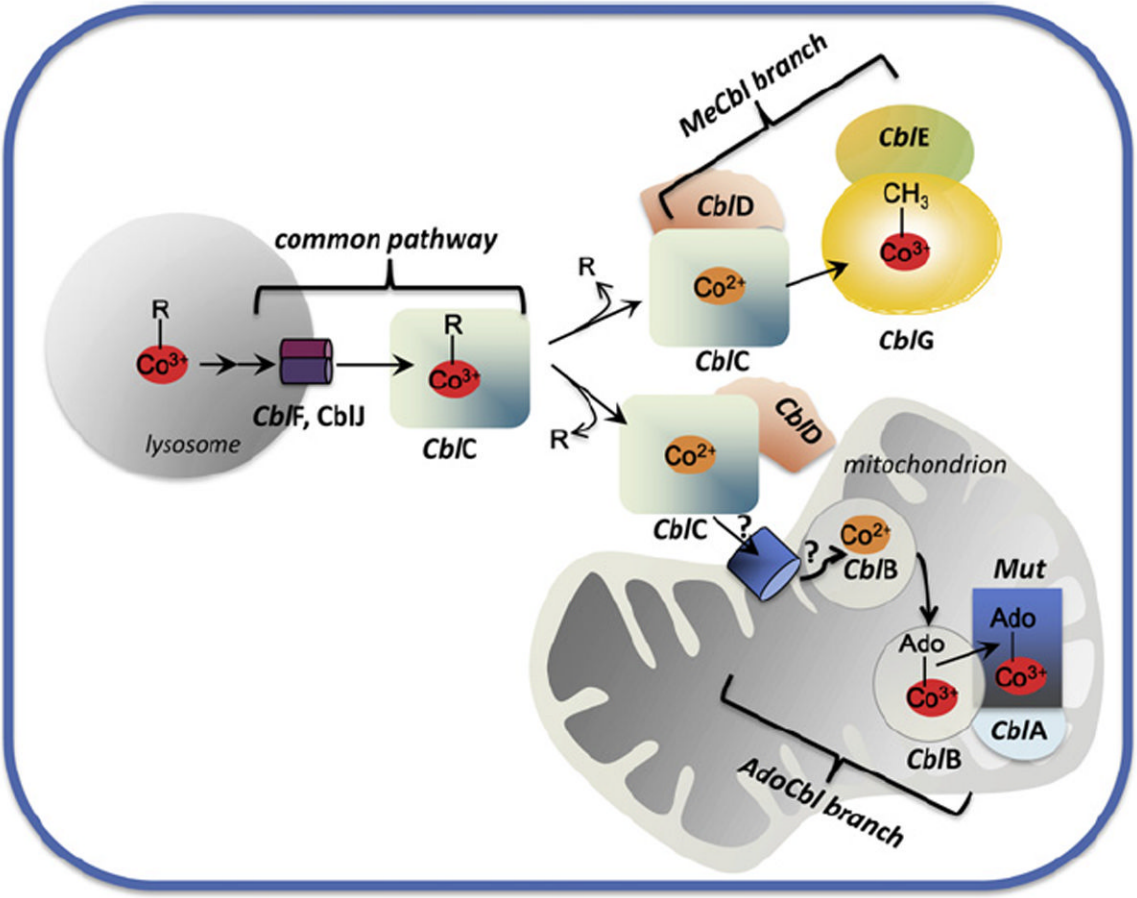

Fig. 1.

Schematic representation of a model for the cobalamin trafficking pathway. Proteins corresponding to the nine genetic complementation groups are designated as CblA-J and Mut (for methylmalonyl-CoA mutase). CblC is proposed to function as the cobalamin donor to cytoplasmic methionine synthase (CblG), which associates with methionine synthase reductase (CblE). We propose that CblD functions as an adapter, facilitating complex formation and/or cofactor transfer from CblC. The mechanism by which B_{12} enters the mitochondrion is not known and a putative transporter is shown in blue for purposes of illustration. The question marks denote the uncertainty in the mechanism for B_{12} import into the mitochondrion and its loading onto CblB. The form of cobalamin bound to CblC after dealkylation is shown as cob(II)alamin for simplicity. We note however that the dealkylation product is cob(I)alamin, which is rapidly oxidized to cob(II)alamin and then HOCbl in vitro. Cob(II)alamin is presumed to be stabilized under the reducing intracellular conditions and is also the product of CblC-catalyzed decyanation of CNCbl.

NIH-PA Author Manuscript

NIH-PA Author Manuscript

NIH-PA Author Manuscript

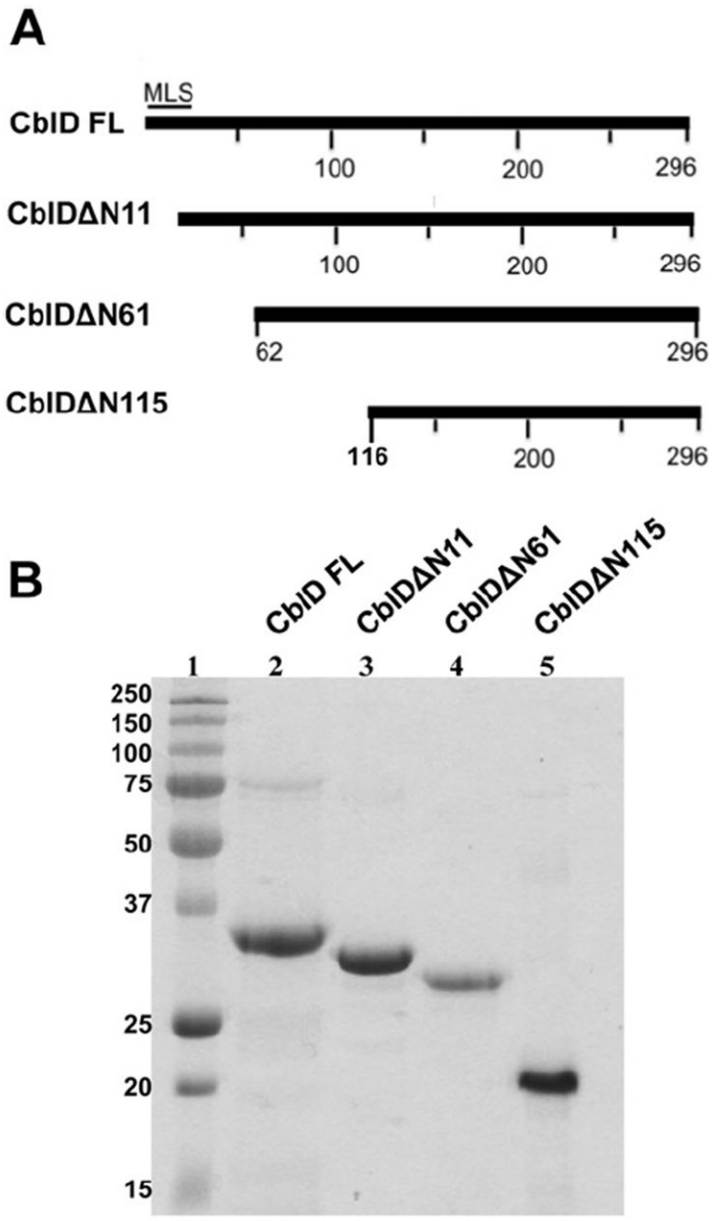

Fig. 2.

Purification of recombinant CblD forms. (A) Boundaries of the CblD constructs used in this study. The predicted mitochondrial leader sequence (MLS) is indicated. (B) SDS-PAGE analysis of protein standards (lane 1) full-length CblD (FL, lane 2), CblD-NΔ11 (lane 3), CblD-NΔ61 (lane 4) and CblD NΔ115 (lane 5). An equal amount of protein (7 μg) was loaded in each lane and visualized by Coomassie blue staining.

NIH-PA Author Manuscript

NIH-PA Author Manuscript

NIH-PA Author Manuscript

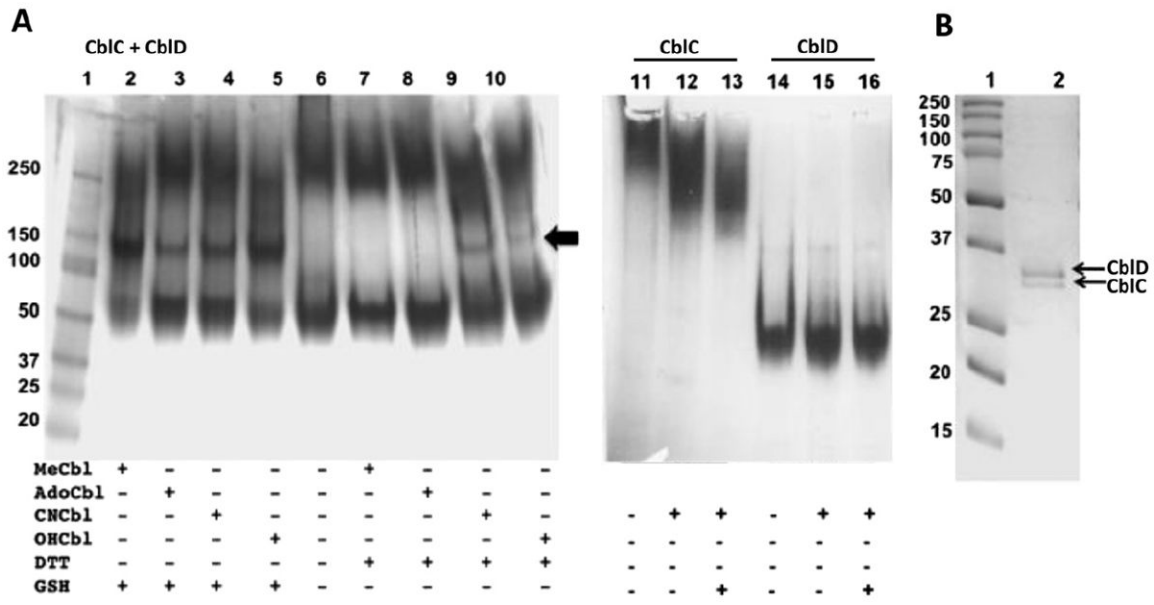

Fig. 3.

Complex formation between CblC and CblD. (A) Formation of a CblC:CblD complex was monitored by native gel electrophoresis on a 4–20% gradient gel as described under Materials and methods. CblC and full-length CblD (FL) were incubated for 30 min at 20 °C in the absence (lane 6) or presence of different B_{12} forms: MeCbl (lanes 2, 7), AdoCbl (lanes 3, 8), CNCbl (lanes 4, 9) and HOCbl (lanes 5, 10). In addition, either glutathione (GSH) (lanes 2–5) or DTT (lanes 7–10) was added to the reaction mixture. A new band representing the CblC:CblD complex (indicated by arrow) was seen and its intensity varied depending on the conditions of the incubation. CblC was loaded either in the absence (lane 11) or presence of CNCbl (lane 12) or CNCbl + glutathione (lane 13). Full-length CblD was loaded in the absence (lane 14) or presence of CNCbl (lane 15) or CNCbl + glutathione (lane 16). (B) The presence of both CblC and full-length CblD in the protein complex seen in (A) was confirmed by excising the band and separating it on a denaturing 12% SDS-PAGE gel.

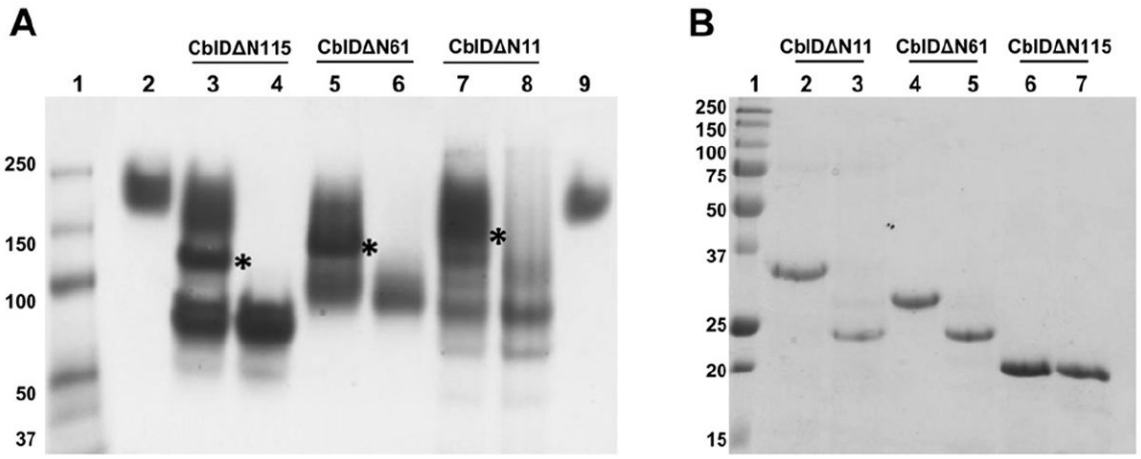

Fig. 4.

Effect of N-terminal deletions on CblD folding and its ability to interact with CblC. (A) Complex formation between CblC (15 μg) and CblD-DΔ11, -ΔN61 and -ΔN115 (15 μg) in the presence of 50 μM MeCbl and 1 mM glutathione (GSH). In each case, CblC mixed with MeCbl and GSH was incubated in the absence (lane 2) or presence of CblD-ΔN11 (lane 7), -ΔN61 (lane 5) and -ΔN115 (lane 3). Control experiments with CblD variants ΔN115 (lane 4), ΔN61 (lane 6) and ΔN11 (lane 8) incubated with MeCbl and GSH only are also shown. CblC + MeCbl + GSH was loaded in lanes 2 and 9. The asterisks denote the CblC·CblD complex. (B) Limited proteolysis of 15 μg CblD-ΔN11, -ΔN61 and -ΔN115 with trypsin (2% w/w) at ambient temperature was performed as described under Materials and methods.

NIH-PA Author Manuscript
NIH-PA Author Manuscript
NIH-PA Author Manuscript

NIH-PA Author Manuscript
NIH-PA Author Manuscript
NIH-PA Author Manuscript

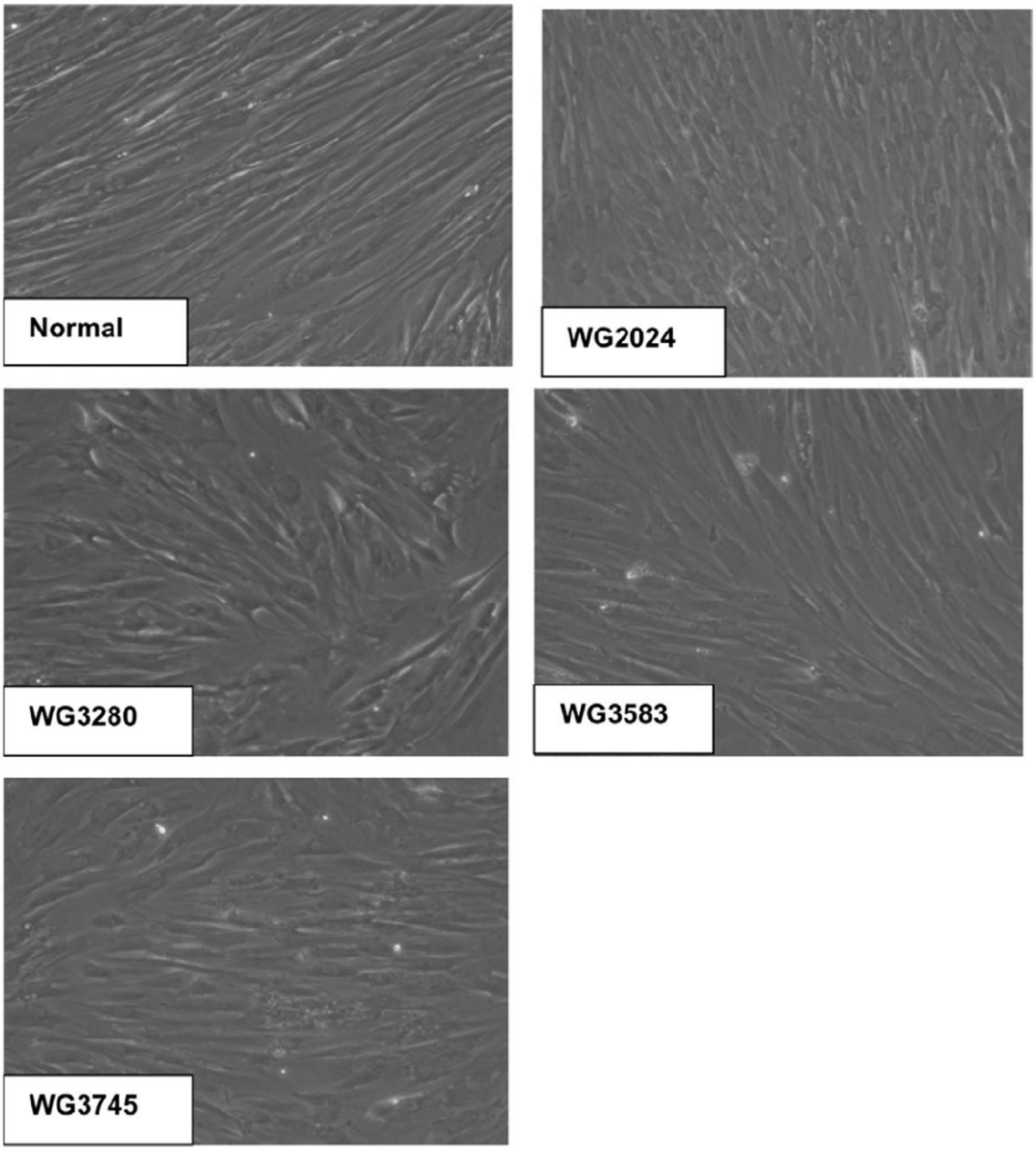

Fig. 5.
Morphology of *cbl*D cell lines. With the exception of WG3583, all *cbl*D cell lines presented morphological differences with respect to the normal cell line. In all cases, the growth was slower for *cbl*D cell lines. However, all cell lines became confluent over time. An enlarged cellular body size and a disrupted fibroblast growth pattern were also evident by phase contrast microscopy. Magnification: 100×.

NIH-PA Author Manuscript

NIH-PA Author Manuscript

NIH-PA Author Manuscript

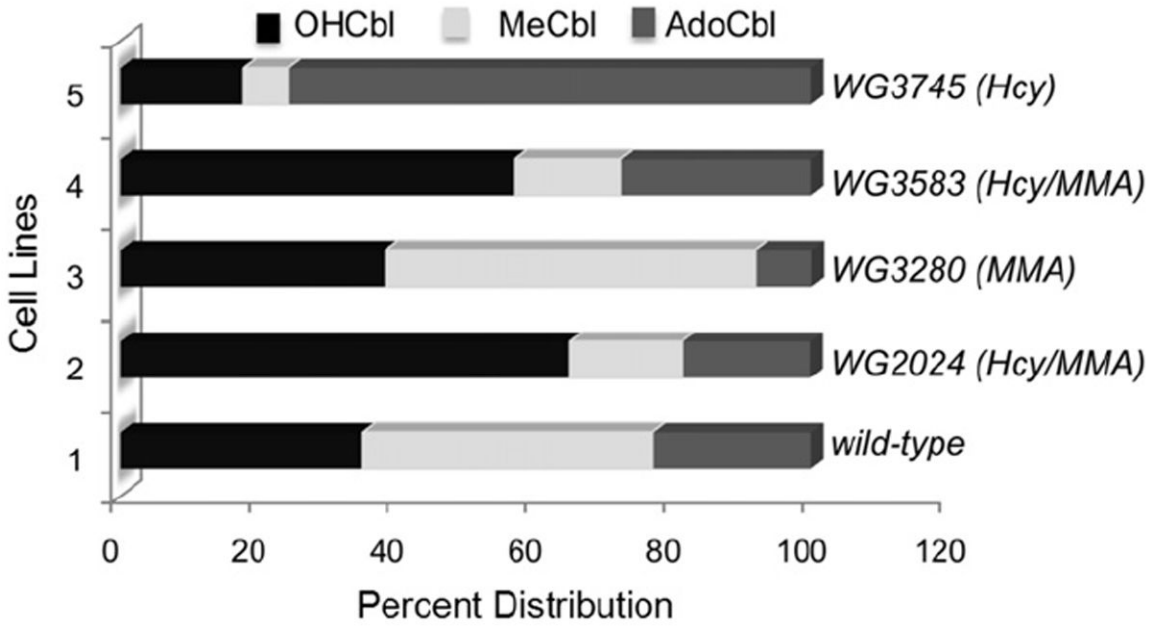

Fig. 6.

Intracellular profile and distribution of [^{57}Co]-cobalamins in normal and *cblD* mutant cell lines after 48 h in culture with [^{57}Co]-MeCbl substrate.

NIH-PA Author Manuscript
NIH-PA Author Manuscript
NIH-PA Author Manuscript

Table 1

Fibroblast cell lines used in this study.

Cell line	Mutation	Phenotype	Age of onset	Reference
HFF	None	Wild type	-	Clevel and Clinic Tissue Culture Core
WG2024	Homozygous 748C>T (p.R250X)	*cbl*D, homocystinuria and methylmalonic aciduria	38 y	[9]
WG3280	c.60insAT (p.L20fsX21) in exon 3 c.455dupC (p.T152fsX162) in exon 5	*cbl*D, methylmalonic aciduria	6 y	[22]
WG3583	Homozygous for c.683C > G (p.S228X) mutation in exon 7	*cbl*D, homocystinuria and methylmalonic aciduria	4.5 months	[22]
WG3745	Homozygous for c.737A > G (p.D246G) in exon 8	*cbl*D, homocystinuria	5 months	[22]

NIH-PA Author Manuscript

NIH-PA Author Manuscript

NIH-PA Author Manuscript

Table 2

Cumulative levels of homocysteine and methylmalonic acid in culture medium after 5 days.[a]

Cell line ID	Phenotype	Homocysteine (μmol/mg protein)	Methylmalonic acid (μmol/mg protein)
HFF	Control	0.016 ± 0.004	0.90 ± 0.12
WG2024	Homocystinuria, methylmalonic aciduria	0.052 ± 0.004	10.1 ± 2.0
WG3280	Isolated methylmalonic aciduria	0.029 ± 0.004	25.1 ± 2.7
WG3583	Homocystinuria, methylmalonic aciduria	0.047 ± 0.006	15.0 ± 1.3
WG3745	Isolated homocystinuria	0.051 ± 0.008	1.56 ± 0.18

[a]The data represent the mean of three independent measurements ± standard deviation.

NIH-PA Author Manuscript NIH-PA Author Manuscript NIH-PA Author Manuscript

Table 3

Total uptake and intracellular distribution of cobalamin derivatives.[a]

Cell line	Total [^{57}Co] retention (fmol Cbl/mg protein)	Intracellular Cbl (fmol/mg protein)			
		HOCbl	AdoCbl	MeCbl	MeCbl:AdoCbl
HFF	0.65 ± 0.06	0.23 ± 0.05 (35%)	0.15 ± 0.02 (23%)	0.27 ± 0.01 (42%)	1.8
WG2024	0.74 ± 0.08	0.48 ± 0.11 (65%)	0.14 ± 0.02 (19%)	0.12 ± 0.03 (16%)	0.86
WG3280	3.58 ± 0.32	1.37 ± 0.22 (38%)	0.30 ± 0.06 (8%)	1.91 ± 0.52 (53%)	6.4
WG3583	0.37 ± 0.03	0.21 ± 0.04 (57%)	0.10 ± 0.02 (27%)	0.06 ± 0.02 16%)	0.6
WG3745	1.07 ± 0.02	0.19 ± 0.03 (18%)	0.81 ± 0.17 (76%)	0.07 ± 0.01 (6%)	0.09

[a]Values represent mean ± standard deviation. Uptake was measured after 48 h of incubation with [^{57}Co]-MeCbl.